Experimental Study on Weldability of Aluminium Alloy AA6063 by Tungsten Inert Gas Welding

Soumojit Dasgupta

Assistant Professor, Department of Mechanical Engineering, JIS College of Engineering, Kalyani- 741235, West Bengal, India

Abstract

Over the years, welding has emerged as an important process for fabrication of engineering components. It has numerous applications in several areas. Gas Tungsten Arc Welding (GTAW) is one of the major welding processes in arc welding. In GTAW, Heat Input and Gas Flow Rate are two major factors during welding process. They have influence on Weld Bead Geometry (depth of penetration, bead width and height of reinforcement) which is an important characteristic in welding process. Weldability measurement is an important criterion in testing the soundness of weld. In this experimental work, AA6063 aluminium alloy was welded using Gas Tungsten Arc Welding (GTAW) process. Heat Input (kJ/mm) and Gas Flow Rate (l/min) were the input factors of three levels each. Central Composite Design (CCD) of Response Surface Methodology (RSM) was applied as the Design of Experiment. Bead geometry parameters were studied for different combinations of the mentioned factors. The influence of each factor on the bead geometry was analysed using ANOVA. It was observed that the maximum depth of penetration was at heat input values of 0.38-0.39 kJ/mm and gas flow rate of 10-13 l/min. Nominal bead width is accepted and was obtained at heat input of 0.43-0.48 kJ/mm and gas flow rate of 17-18 l/min. Nominal positive reinforced height is acceptable and this was obtained at heat input value of 0.38-0.385 kJ/mm and gas flow rate of 17.8-18 l/min.

Keywords- Aluminium alloy, Bead geometry, GTAW, weldability, Central Composite Design

1. Introduction

The process of joining metals by Tungsten Inert Gas (TIG) welding or Gas Tungsten Arc welding (GTAW) has emerged as an interesting area of research. Among metals, aluminium and its alloys find huge application owing to their lightness and strength to weight ratio. Thus, welding of aluminium alloys and their quality is very important. Numerous

experimental investigations were conducted on welding of aluminium alloys using TIG welding.

Numerous researches have been conducted in this area. Lakshman Singh et. al [1] investigated on TIG welding parameters and their effect on tensile strength of 5083 Al-alloy specimens. The input parameters considered were welding current, gas flow rate and welding speed. It was inferred that with increasing weld speed, tensile strength increased initially. However, after reaching optimum value, the strength declined. Wrought aluminium AA8006 alloy was welded using GTAW process by T Sathish et. al [2]. Input parameters of welding speed, base current and peak current at three levels were used following Taguchi L9 orthogonal array. Investigations were performed to test surface hardness, tensile strength and impact strength. Results were evaluated statistically and described. In another interesting experimental work by Gurmeet Singh et. al [3], comparative study was made on results of friction stir welding and TIG welding on 6082-T6 Aluminium alloy. The effects of both welding processes on mechanical and metallurgical properties were done. Studies revealed that friction stir welding produced better mechanical properties compared to TIG welding. Microstructure analysis revealed that friction stir welding produced fine and equiaxed grains, while TIG welding produced coarse grains. Pankaj C Patil and RD Shelke [4] reviewed on effects of welding parameters by TIG welding of aluminium alloys. Effect of Welding current, gas flow rate and welding speed was analysed on aluminium alloy 7005 grade. Effect of input factors on tensile strength and hardness were analysed. Aleksandra Koprivica et. al [5] attempted a comparative study of TIG, MIG and FSW welding on AA6082-T6 aluminum alloy. Investigation on microstructure and mechanical properties of AA6061 aluminium alloy by TIG and MIG welding was done by Saurabh Kumar Khotiyan and Sandeep Kumar [6]. It was observed that superior tensile strength, hardness, impact strength and microstructure were produced compared to MIG welding. S Shanavas and J Edwin Raja Dhas [7] investigated on effect of input parameters of TIG welding on weld quality of AA 5052 H32 aluminium alloy. Also, mechanical characteristics of the welded joints were compared to joints produced by friction stir welding. Weld current and gas flow rates were the input variables. The weld strength was measured w.r.t. ultimate tensile strength. A comparative study on weldability and mechanical properties of 6063 T6 aluminium alloy by TIG welding and friction stir welding (FSW) was performed by Parminder Singh et. al [8] and Navneet Khanna et. al [9]. It was observed that thickness of heat affected zone of weld bead by FSW was narrower compared to TIG welding. Also, FSW produced improved tensile strength. Results revealed lower residual stress for FSW and prevention of fusion defects. Ario Sunar Baskoro et. al [10] examined the effects of TIG welding parameters on macrostructure, microstructure, and mechanical properties of AA6063-T5 with controlled intermittent wire feeding. Microstructure revealed the segregation at the central region with high density eutectic phase. Also, it was observed that magnesium content was higher at the central region compared to outside portion. SEM analysis concluded presence of columnar structure in dilution boundaries, which proved that fast cooling resulted due to insertion of filler wire. Dissimilar welding of aluminium alloys AA6061 and AA7075 by TIG welding using different filler metals such as ER4043 and ER5356 was attempted by Mahadzir Ishak et. al [11]. Visual inspection, microstructure and hardness were studied for both the filler materials. Depth of penetration of 1.74mm was produced by ER5356 compared to 0.9mm by ER4043. Study of microstructure at various zones of dissimilar welding was performed. Hardness values of weld beads by ER5356 filler was higher compared to ER4043. It was concluded

that TIG welding using ER5356 filler produced improved weld. Effect of heat input, porosity and post-weld heat treatment mechanical properties and microstructure of TIG welded joints of AA6082-T6 was analysed by Bo Wang et. al [12]. Bead-on-plate TIG welding of Al 7075 aluminium alloy was performed by S. Aravind and A. Daniel Das [13]. Experiments were performed using weld current, weld speed and weld time as the input factors according to Response Surface Methodology design of experiment. Weld bead strength was measured using tensile test. In another experiment by B Narenthiran et. al [14], TIG welding on aluminium alloy AA6063 was performed using zirconated tungsten electrode and aluminium alloy filler material. Input factors considered were weld current, weld speed and arc gap and tensile strength of the weld was the response. Rajiv Kumar et. al [15] experimented on comparative weld performance of conventional TIG welding and activated TIG welding on AA6063 T6 aluminium alloy. Results showed that ATIG welding produced better penetration and less bead width compared to conventional TIG welding. Also, the former produced better tensile strength than latter. Failure method was ductile and brittle for ATIG welding and conventional TIG welding respectively. An attempt to perform TIG-AC welding on Aluminium Alloy AA 6063-T6 was done by Jonny Max Catarino et. al [16]. Simple plate deposition with rectangular wave was performed with variation of both current and time of positive polarity of electrode. Results showed that decrease in positive wave time decreased depth of penetration and bead width. This was attributed to selection of time and frequency used. In another similar type of experiment, M. A. R. Yarmuch and B. M. Patchett [17] investigated on the effect of electrode positive polarity during unbalanced square wave AC welding of aluminium alloys with GTAW process on depth of penetration and bead width. The responses increased with increase in positive polarity. Dong Peng et. al investigated on microstructure and mechanical properties of TIG welded 6061-T6 alloy under ageing treatment and different conditions of heat input. Observation of microstructure, micro hardness and tensile test was performed. Observations showed that increasing heat input resulted in increased width of heat affected zone (HAZ) and coarse grains in fusion zone. Hardness of HAZ decreased, while hardness of fusion zone (FZ) decreased initially and then increased. On the other hand, low heat input resulted in low ultimate tensile strength of welded joint.

2. Experiment

2.1 GTAW Process Parameters

The factors considered for GTAW of AA6063 are-

i) Heat Input   ii) Gas Flow Rate

Heat Input

Heat input is a crucial process parameter in TIG welding that directly influences the quality and characteristics of the weld. Heat input refers to the amount of energy transferred to the base material and the filler metal during the welding process. It is expressed in terms of energy per unit length, measured in kilojoules per millimeter (kJ/mm).

Gas Flow Rate

GTAW requires the use of shielding gas, like argon or a mixture of argon and helium, to protect the weld pool and tungsten electrode from atmospheric contamination. The gas flow rate is the rate at which the shielding gas is supplied to the welding zone. It is usually measured in litres per minute (l/min).

2.2 Limits of the GTAW process parameters

Trial runs were conducted for determining the range of values for the process parameters. Finally, the following levels were considered.

Factors	Level 1 (-1)	Level 2 (0)	Level 3 (+1)
Heat Input (kJ/mm)	0.380	0.430	0.490
Gas flow rate (l/min)	10	14	18

Table 1: Process parameters and their levels

The value of heat input is calculated from the following equation-

Heat Input = ή x V x I/1000 x s,
where
ή = Weld efficiency, generally considered as 0.75 or 75%
V= Weld voltage (Volt)
I = Weld current (Ampere)
s= weld speed (mm/s)

2.3 Design of Experiment

Design of experiment holds a key factor in determining the complete sequence of experimental process. It is a statistical tool that helps in determining the combination of process parameters during the experimentation. Here, Central Composite Design (CCD) of Response Surface Methodology is the design of experiment.

2.4 Developing the experimental design matrix

Experiments were performed involving two factors and three levels each. According to Central Composite design of experiment, thirteen numbers of experiments was performed as shown in Table 2.

Sl. No.	Run Order	Current (Coded Value)	Gas Flow rate (Coded Value)
1.	2	-1	-1
2.	7	+1	-1
3.	10	-1	+1
4.	4	+1	+1
5.	12	-1	0
6.	9	+1	0
7.	5	0	-1
8.	13	0	+1
9.	1	0	0
10.	3	0	0
11.	6	0	0
12.	8	0	0
13.	11	0	0

Table 2: Experimental conditions for GTAW welding

2.5 Experimentation

GTAW process was performed on AA6063 aluminium alloy with plate thickness 10 mm using TIG welding machine, with the following specification as shown in Table 3.

TIG welding machine	Model: QNFC 28, Standard- EN60974-2, EN60974-10, ClassA Manufactured by Carl Cloos Schweiss Technik GmBH, European Union
Current	152 A, 194 A, 215 A (AC)
Welding Speed	3.25 mm/sec
Shielded Gas	High purity Argon Gas
Electrode	Φ 3.2 mm Thoriated Tungsten electrode
Filler material	ER4043, Ø 2 mm

Table 3: TIG welding machine details

Shielded Gas - High purity Argon

Electrode material - Thoriated Tungsten electrode of diameter 3.2 mm

Filler material - ER4043 of diameter 2 mm

The complete setup of the TIG welding machine is illustrated in Figure 1.

Figure 1: TIG welding machine setup

2.6 Process

Initially, AA6063 aluminium alloy plates of dimensions 40 mm x 50 mm x15 mm were cut into twenty-six (26) pieces, i.e. for thirteen welded joints. Then, cleaning of base materials were performed followed by edge preparation. Double-V groove edge preparation was made. Finally, GTAW was done resulting in 13 pairs of weldments. During welding, two input factors were considered as input, i.e. Heat Input and Gas Flow Rate. After welding, output parameters (responses) in the form of weld bead geometry, i.e. depth of penetration, bead width and height of reinforcement was measured. Typical visual outputs after welding is summarized in Table 4.

Sl. No.	Weldment photo	Visual Inspection Remarks
1.		Minute pin holes on bead surface.
2.		Minute pin holes on bead surface.
3.		Two pin holes on bead surface.
4.		Even weld profile throughout.

Table 4: Typical weld bead profiles with visual inspection remarks

3. Results and Discussion

As was discussed, weld bead geometry, i.e. depth of penetration, bead width and height of reinforcement were measured. The detailed results are summarized in Table 5.

Sl. No.	Current (A)		Voltage	Weld Speed (mm/sec)	Heat Input (kJ/mm)	Gas Flow Rate (lit/min)	Depth Of Penetration (mm)	Bead Width(mm)	Height of reinforcement (mm)
	c.c.c	o.c.c							
1	100	100	15.7	3.8	0.380	10	8.23	14.72	6.89
2	140	140	14.2	3.8	0.490	10	5.87	12.56	5.78
3	100	100	14.4	3.8	0.380	18	8.26	14.34	7.22
4	139	140	13.7	3.8	0.490	18	5.45	9.63	4.65
5	100	100	13.9	3.8	0.380	14	9.56	15.23	4.87
6	140	140	16.02	3.8	0.490	14	3.73	15.42	11.34
7	120	120	16.3	3.8	0.490	10	9.28	14.76	5.76
8	120	120	14.4	3.8	0.430	18	5.42	12.53	7.33
9	120	120	14.5	3.8	0.430	14	3.73	11.64	9.56
10	120	120	13.9	3.8	0.430	14	4.42	13.78	10.15
11	120	120	14.2	3.8	0.430	14	4.62	12.65	9.44
12	120	120	14.5	3.8	0.430	14	3.65	11.34	8.56
13	120	120	13.1	3.8	0.430	14	3.93	12.22	8.21

Table 5: Experimental results of bead geometry

3.1 Analysis of Results

i) Depth of Penetration

Considering results of depth of penetration, Contour plot and Surface plot were generated as shown in Figure 2 and Figure 3.
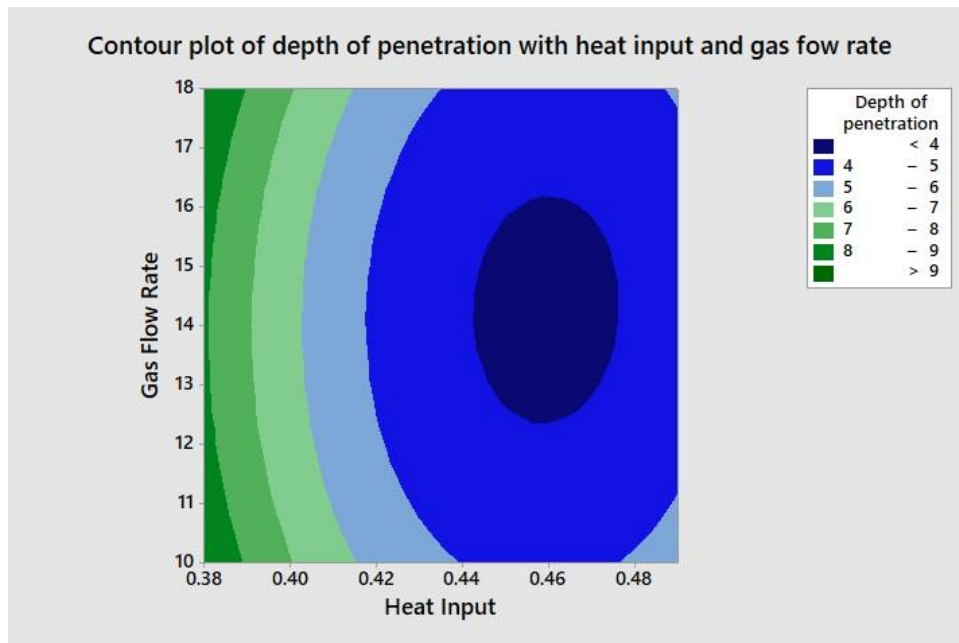

Figure2: Contour Plot of Depth of Penetration with Heat Input & Gas Flow Rate
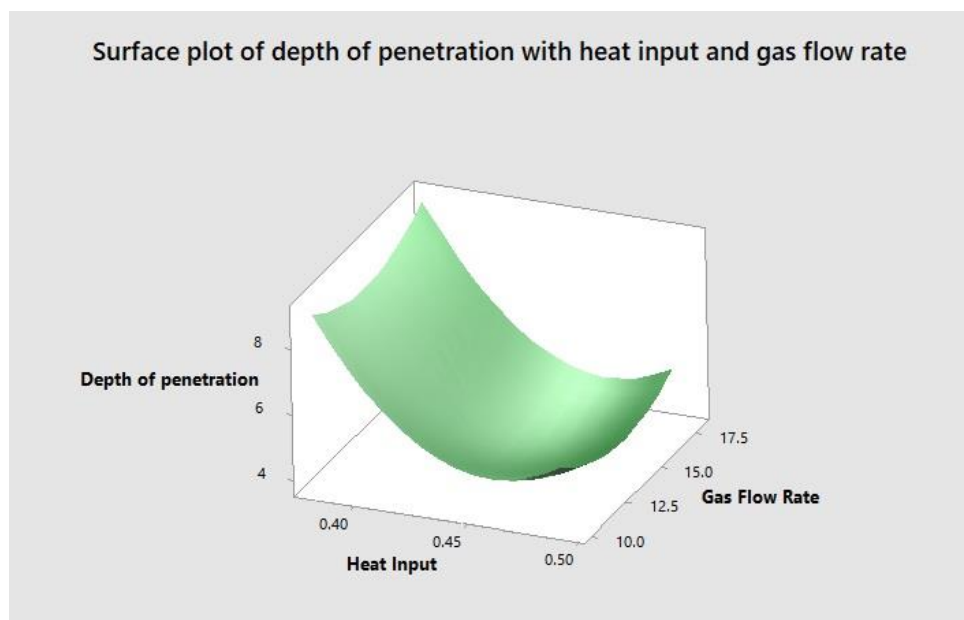

Figure3: Surface Plot of Depth of Penetration with Heat Input & Gas Flow Rate

According to the contour plot as shown in Figure 2, depth of penetration was measured at constant heat inputs 0.4 kJ/mm, 0.44kJ/mm and 0.48 kJ/mm corresponding to gas flow rates of 11 l/min, 14 l/min and 17 l/min. Thus, at 0.4 kJ/mm heat input and the mentioned gas flow rates, depth of penetration were measured within range 6-7 mm. Similarly, at constant heat input of 0.44kJ/mm and the previously mentioned gas flow rates, depth of penetration were measured within range 4-5mm. Finally, at 0.48 kJ/mm heat input and the mentioned gas flow rates, the penetration depth were obtained within 5-6 mm, and 4-5mm respectively. Correspondingly, depth of penetration were measured at constant gas flow rates of 11 l/min, 14 l/min and 17 l/min w.r.t. heat input values of 0.4 kJ/mm, 0.44 kJ/mm and 0.48 kJ/mm. Thus, at 11 l/min gas flow rate and the mentioned heat inputs, depth of penetration was measured within 4-8 mm. Similarly, at constant gas flow rate of 14 l/min and the previously mentioned heat inputs, depth of penetration were measured within range <4-8 mm respectively. Finally, at 17 l/min gas flow rate and the mentioned heat inputs, penetration depth were obtained within 5->9 mm. The surface plot as in Figure 3, reiterated similar findings.

Analysis of variance (ANOVA) was performed to evaluate the influence of each parameter on the responses. Table 6 shows the ANOVA of depth of penetration with heat input and gas flow rate.

Analysis of Variance

Source	DF	Adj SS	Adj MS	F-Value	P-Value
Model	5	40.7435	8.1487	11.39	0.003
Linear	2	20.1920	10.0960	14.11	0.004
Heat Input	1	20.1667	20.1667	28.18	0.001
Gas Flow Rate	1	0.0253	0.0253	0.04	0.856
Square	2	20.5008	10.2504	14.33	0.003
Heat Input*Heat Input	1	11.8542	11.8542	16.57	0.005
Gas Flow Rate*Gas Flow Rate	1	1.9801	1.9801	2.77	0.140
2-Way Interaction	1	0.0506	0.0506	0.07	0.798
Heat Input*Gas Flow Rate	1	0.0506	0.0506	0.07	0.798
Error	7	5.0088	0.7155		
Lack-of-Fit	3	4.2722	1.4241	7.73	0.139
Pure Error	4	0.7366	0.1841		
Total	12	45.7523			

Model Summary

S	R-sq
0.845898	90.00%

Table 6: ANOVA Table of Depth of Penetration

The ANOVA table shows that Linear P-values for heat input is less than 0.05, but for gas flow rate is more than 0.05. Thus, only heat input has significant contribution on the depth of penetration.

Also, the R-sq value of 90% is significantly higher, which denotes that the results are acceptable.

ii) Bead Width

Considering results of bead width, Contour plot and Surface plot were generated as shown in Figure 4 and Figure 5.
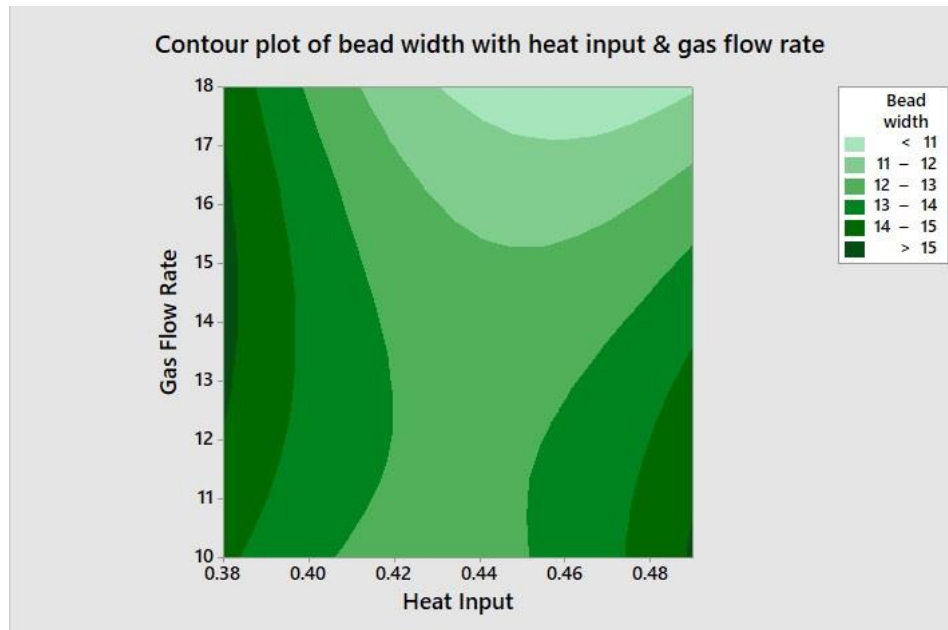

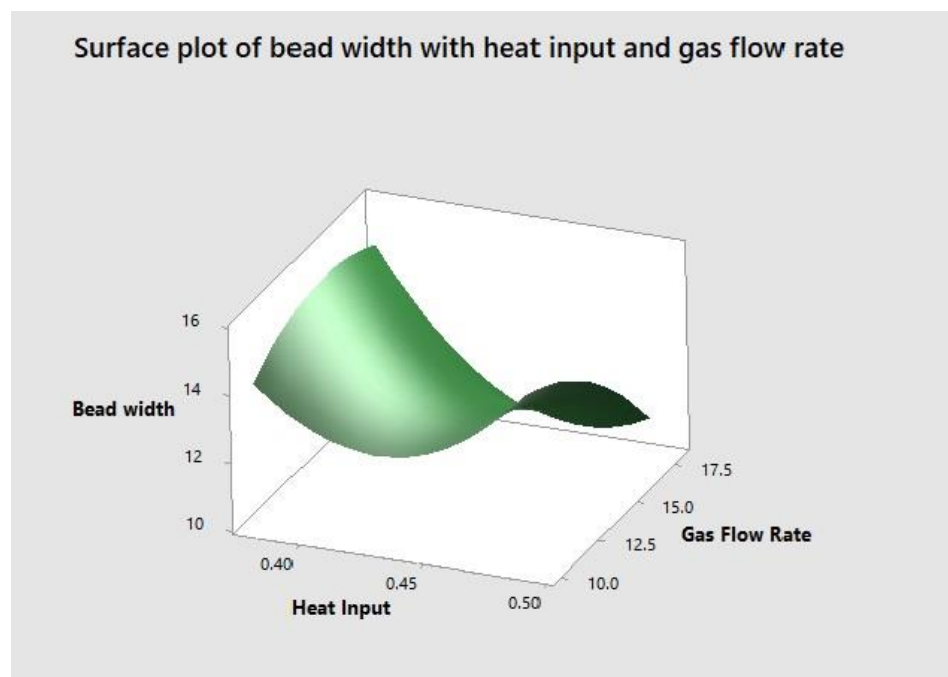**Figure 4: Contour Plot of Bead Width with Heat Input & Gas Flow Rate**

Figure 5: Surface Plot of Bead Width with Heat Input & Gas Flow Rate

According to the contour plot as shown in Figure 4, bead width was measured at constant heat inputs 0.4 kJ/mm, 0.44kJ/mm and 0.48 kJ/mm corresponding to gas flow rates of 11 l/min, 14 l/min and 17 l/min. Thus, at 0.4 kJ/mm heat input and the mentioned gas flow rates, bead width were measured within range 13-14 mm. Similarly, at constant heat input of

0.44kJ/mm and the previously mentioned gas flow rates, bead width were measured within range <11-13mm. Finally, at 0.48 kJ/mm heat input and the mentioned gas flow rates, the bead width were obtained within <11-15. Correspondingly, bead width were measured at constant gas flow rates of 11 l/min, 14 l/min and 17 l/min w.r.t. heat input values of 0.4 kJ/mm, 0.44 kJ/mm and 0.48 kJ/mm. Thus, at 11 l/min gas flow rate and the mentioned heat inputs, bead width was measured within <11-15 mm. Similarly, at constant gas flow rate of 14 l/min and the previously mentioned heat inputs, bead width were measured within range 12-15 mm. Finally, at 17 l/min gas flow rate and the mentioned heat inputs, bead width was obtained within 12-15 mm. The surface plot as in Figure 5, reiterated similar findings.

Analysis of variance (ANOVA) was performed to evaluate the influence of each parameter on the responses. Table 7 shows the ANOVA of bead width with heat input and gas flow rate.

Analysis of Variance

Source	DF	Adj SS	Adj MS	F-Value	P-Value
Model	5	25.214	5.043	2.87	0.101
Linear	2	8.460	4.230	2.41	0.160
Heat Input	1	3.345	3.345	1.90	0.210
Gas Flow Rate	1	5.115	5.115	2.91	0.132
Square	2	11.113	5.556	3.16	0.105
Heat Input*Heat Input	1	11.112	11.112	6.32	0.040
Gas Flow Rate*Gas Flow Rate	1	1.655	1.655	0.94	0.364
2-Way Interaction	1	5.641	5.641	3.21	0.116
Heat Input*Gas Flow Rate	1	5.641	5.641	3.21	0.116
Error	7	12.306	1.758		
Lack-of-Fit	3	8.241	2.747	2.70	0.180
Pure Error	4	4.065	1.016		
Total	12	37.520			

Model Summary

S	R-sq
1.32589	87.20%

Table 7: ANOVA Table of bead width

The ANOVA shows that Linear P-values for both heat input and gas flow rate are above 0.05 and thus are insignificant. However, the square interaction of heat input is less than 0.05 and thus has impact on bead width.

Also, the R-sq value of 87.20% is significantly higher, which denotes that the results are acceptable.

iii) Height of reinforcement

Considering results of height of reinforcement, Contour plot and Surface plot were generated as shown in Figure 6 and Figure 7.
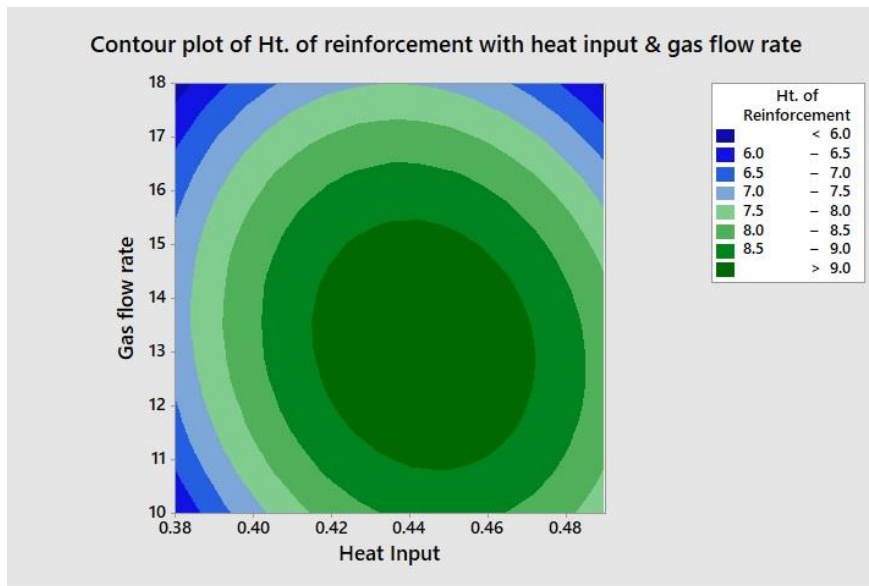
Figure 6: Contour Plot of Height of reinforcement with Heat Input & Gas Flow Rate
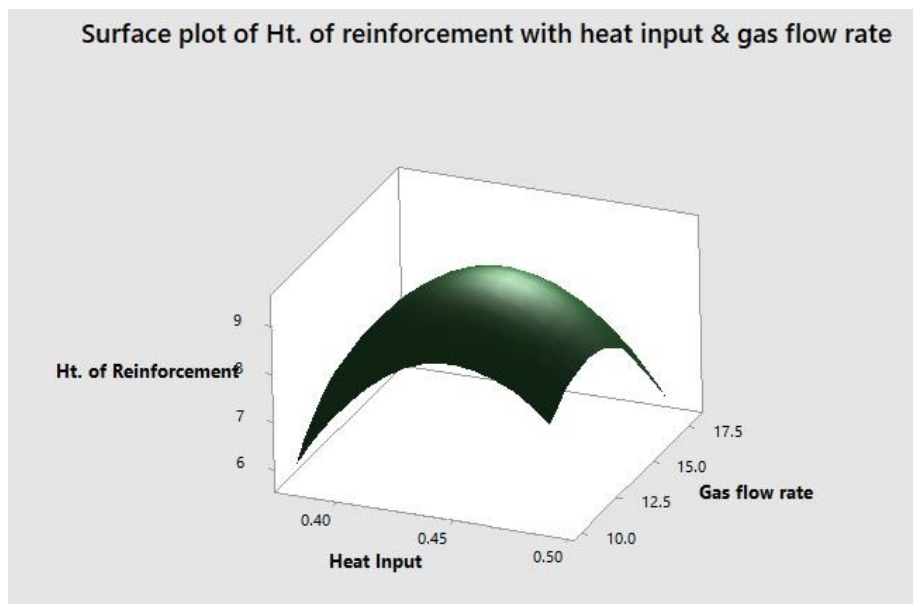

Figure 7: Surface Plot of Height of reinforcement with Heat Input & Gas Flow Rate

According to the contour plot as shown in Figure 6, height of reinforcement was measured at constant heat inputs 0.4 kJ/mm, 0.44kJ/mm and 0.48 kJ/mm corresponding to gas flow rates of 11 l/min, 14 l/min and 17 l/min. Thus, at 0.4 kJ/mm heat input and the mentioned gas flow rates, height of reinforcement were measured within range 7-8.5 mm. Similarly, at constant heat input of 0.44kJ/mm and the previously mentioned gas flow rates, height of reinforcement was measured within range 7.5->9 mm. Finally, at 0.48 kJ/mm heat input and the mentioned gas flow rates, the height was obtained within 8-6mm. Correspondingly, height of reinforcement were measured at constant gas flow rates of 11 l/min, 14 l/min and 17 l/min w.r.t. heat input values of 0.4 kJ/mm, 0.44 kJ/mm and 0.48 kJ/mm. Thus, at 11 l/min gas flow rate and the mentioned heat inputs, height of reinforcement was measured within

6.5-9 mm. Similarly, at constant gas flow rate of 14 l/min and the previously mentioned heat inputs, height of reinforcement was measured within range 7->9 mm and then again it decreased. Finally, at 17 l/min gas flow rate and the mentioned heat inputs, height of reinforcement was obtained within 6.5-8.5 mm and then it again decreased. The surface plot as in Figure 7, reiterated similar findings.

Analysis of variance (ANOVA) was performed to evaluate the influence of each parameter on the responses. Table 8 shows the ANOVA of bead width with heat input and gas flow rate.

Analysis of variance

```
Analysis of Variance

Source                          DF   Adj SS   Adj MS   F-Value  P-Value
Model                            5  30.9061   6.1812     1.63    0.268
  Linear                         2   3.1453   1.5726     0.42    0.676
    Heat input                   1   2.2940   2.2940     0.61    0.002
    Gas flow rate                1   0.8513   0.8513     0.22    0.050
  Square                         2  26.4036  13.2018     3.48    0.089
    Heat input*Heat input        1   0.5461   0.5461     0.14    0.715
    Gas flow rate*Gas flow rate  1  19.5371  19.5371     5.16    0.057
  2-Way Interaction              1   1.3572   1.3572     0.36    0.568
    Heat input*Gas flow rate     1   1.3572   1.3572     0.36    0.568
Error                            7  26.5187   3.7884
  Lack-of-Fit                    3  23.9270   7.9757    12.31    0.217
  Pure Error                     4   2.5917   0.6479
Total                           12  57.4248


Model Summary

      S     R-sq
1.94638   93.82%
```

Table 8: ANOVA Table of height of reinforcement

The ANOVA table shows that Linear P-values for both heat input and gas flow rate is less than or equal to 0.05. Thus, both heat input and gas flow rate have significant contribution on the height of reinforcement.

Also, the R-sq value of 93.82% is significantly higher, which denotes that the results are acceptable.

Conclusion

In this experimental investigation on the weldability of AA6063 aluminium alloy by using Tungsten Inert Gas welding process, Central Composite Design of the Response Surface Methodology was used as the design of experiment. Argon (99.9% pure) was used as the shielding gas. ER4043 rod was applied as the filler material of 2mm diameter. From the results, it is evident that both Heat Input and Gas Flow Rate have significant contribution on

the Weld Bead Geometry parameters, i.e. depth of penetration, bead width and height of reinforcement.

The following inferences were concluded-

i)   Maximum depth of penetration was at heat input values of 0.38-0.39 kJ/mm and gas flow rate of 10-13 l/min.

ii) Nominal bead width is accepted and was obtained at heat input of 0.43-0.48 kJ/mm and gas flow rate of 17-18 l/min.

iii) Nominal positive reinforced height is acceptable and this was obtained at heat input value of 0.38-0.385 kJ/mm and gas flow rate of 17.8-18 l/min.

iv) ANOVA table shows that Linear P-values for heat input is less than 0.05, but for gas flow rate is more than 0.05. Thus, only heat input has significant contribution on the depth of penetration.

v)   ANOVA shows that Linear P-values for both heat input and gas flow rate are above 0.05 and thus are insignificant. However, the square interaction of heat input is less than 0.05 and thus has impact on bead width.

vi) ANOVA table shows that Linear P-values for both heat input and gas flow rate is less than or equal to 0.05. Thus, both heat input and gas flow rate have significant contribution on the height of reinforcement.

5. References

[1] Lakshman Singh, Rajeshwar Singh, Naveen Kumar Singh, Davinder Singh, Pargat Singh; An evaluation of TIG welding parametric influence on tensile strength of 5083 aluminium alloy; Int. J. Mech. Aerospace, Ind. Mechatronics Eng 7 (11), 1262-1265, 2013

[2] T Sathish, S Tharmalingam, V Mohanavel, KS Ashraff Ali, Alagar Karthick, M Ravichandran, Sivanraju Rajkumar; Weldability investigation and optimization of process variables for TIG-welded aluminium alloy (AA 8006); Advances in Materials Science and Engineering 2021, 1-17, 2021

[3] Gurmeet Singh, Amardeep S Kang, Kulwant Singh, Jagtar Singh; Experimental comparison of friction stir welding process and TIG welding process for 6082-T6 Aluminium alloy; materials today: proceedings 4 (2), 3590-3600, 2017

[4] Pankaj C Patil, RD Shelke; Review on welding parameter effects on TIG welding of aluminium alloy; International Journal of Engineering Research and General Science 3 (3), 1479-1486, 2015

[5] Aleksandra Koprivica, Darko Bajić, Nikola Šibalić, Milan Vukčević; Analysis of welding of aluminium alloy AA6082-T6 by TIG, MIG and FSW processes from technological and economic aspect; Machines. Technologies. Materials. 14 (5), 194-198, 2020

[6] Saurabh Kumar Khotiyan, Sandeep Kumar; Investigation of microstructure and mechanical properties of TIG and MIG welding using aluminium alloy; International Journal of Education and Research Review 1 (5), 90-96, 2014

[7] S Shanavas, J Edwin Raja Dhas; Weldability of AA 5052 H32 aluminium alloy by TIG welding and FSW process–a comparative study; IOP Conference Series: Materials Science and Engineering 247 (1), 012016, 2017

[8] Parminder Singh, SK Gandhi, Harshdeep Shergill; Comparative study of friction stir and TIG welding for aluminium 6063-T6; International Journal of Engineering Research & Technology (IJERT) 1, 1-6, 2012

[9] Navneet Khanna, Bhavesh Chaudhary, JayAirao, Gaurav Dak, Vishvesh J Badheka; Experimental comparison of TIG and friction stir welding process for AA6063-T6 aluminium alloy; Innovations in infrastructure: proceedings of ICIIF 2018, 619-628, 2019

[10] Ario Sunar Baskoro, Mohammad Azwar Amat, AlfianIbnuPratama, Gandjar Kiswanto, WinartoWinarto; Effects of tungsten inert gas (TIG) welding parameters on macrostructure, microstructure, and mechanical properties of AA6063-T5 using the controlled intermittent wire feeding; The International Journal of Advanced Manufacturing Technology 105, 2237-2251, 2019

[11] Mahadzir Ishak, Nur Fakhriah Mohd Noordin, Luqman Shah; Feasibility study on joining dissimilar aluminum alloys AA6061 and AA7075 by Tungsten inert gas (TIG), Jurnal Teknologi (Sciences & Engineering) 75:7 (2015) 79–84.

[12] Bo Wang, Songbai Xue, Chaoli Ma, Jianxin Wang, Zhongqiang Lin; Effects of porosity, heat input and post-weld heat treatment on the microstructure and mechanical properties of TIG welded joints of AA6082-T6; Metals 7 (11), 463, 2017

[13]S. Aravind and A.Daniel Das, "An examination on GTAW samples of 7-series aluminium alloy using response surface methodology," *Materials Today*, vol. 37, pp. 1–7, 2020.

[14] B Narenthiran, R Vignesh, A Daniel Das, N Subramani; Parametric evaluation of AA6063 TIG welded samples using Taguchi method; AIP Conference Proceedings 2446 (1), 2022

[15] Rajiv Kumar, SC Vettivel, Harmesh Kumar Kansal; Effect of SiO2 flux on the depth of penetration, microstructure, texture and mechanical behaviour of AA6063 T6 aluminium alloy using activated TIG welding; Bulletin of the Polish Academy of Sciences Technical Sciences, e136215-e136215, 2021

[16] Jonny Max Catarino, Valter Roberto Brito Celestino, MAP Bueno, IDD Valarelli, Manoel Cléber de Sampaio Alves, LER Pereira; Effects of macro and microstructure of aluminium alloy AA 6063-T6 with TIG-AC welding process with unbalanced rectangular wave; Key Engineering Materials 735, 65-69, 2017

[17] Yarmuch, M., Patchett, B. M., 2007, "Variable AC polarity GTAW fusion behavior in 5083 aluminum", Welding Journal, 86, pp. 196-200.

[18] Dong Peng, Jun Shen, Qin Tang, Cui-ping Wu, Yan-bing Zhou; Effects of aging treatment and heat input on the microstructures and mechanical properties of TIG-welded 6061-T6 alloy joints; International Journal of Minerals, Metallurgy, and Materials 20, 259-265, 2013